Integral Experiment Request 554 CED-1 Summary Report

Mathieu N. Dupont
David Ames
Gary Harms
William J. Marshall
Marco T. Pigni

October 2022

![Oak Ridge National Laboratory logo]

ORNL/TM-2022/2682

Nuclear Energy and Fuel Cycle Division

United States Department of Energy
National Nuclear Security Administration
Nuclear Criticality Safety Program

INTEGRAL EXPERIMENT REQUEST 554
CED-1 SUMMARY REPORT

Mathieu N. Dupont
David Ames
Gary Harms
William J. Marshall
Marco Pigni

For the Critical and Subcritical Experiment Design Team (C$_E$dT)

Mathieu N. Dupont (ORNL), CEdT Lead
David Ames (SNL), Experiment Member
Gary A. Harms (SNL), additional Member
William J. Marshall (ORNL), Methods Member
Marco T. Pigni (ORNL), NDAG Member

October 2022

CONTENTS

LIST OF FIGURES

LIST OF TABLES

ABBREVIATIONS

7uPCX	Seven Percent Critical Experiments
ACRR	Annular Core Research Reactor
BUCCX	Burnup Credit Critical Experiment
CED	Critical Engineering Decision
$C_E dT$	Critical Subcritical Experiment Design Team
CT	Computerized Tomography
DOE	US Department of Energy
EALF	Energy corresponding to the Average Lethargy of neutrons causing Fission
ENDF	Evaluated Nuclear Data File
HFIR	High Flux Isotope Reactor
ICSBEP	International Criticality Safety Benchmark Evaluation Project
IER	Integral Experiment Request
MSC	Manufacturing Sciences Corporation
MSTD	Materials Science and Technology Division
NCSP	Nuclear Criticality Safety Program
ORNL	Oak Ridge National Laboratory
SNL	Sandia National Laboratories
SNS	Spallation Neutron Source
SPRF/CX	Sandia Pulsed Reactor Facility/Critical Experiments

ACKNOWLEDGMENTS

SUMMARY

This Critical Engineering Decision 1 report for the Integral Experiment Request 554 describes the effects of adding a commercially available neutron absorber material to a known light-water low-enriched uranium assembly. The assembly in question is the Seven Percent Critical Experiments at Sandia National Laboratories. The neutron absorber plates considered for the experiment are called Boralcan, which are made of boron carbide (B_4C) particles embedded in 1100 aluminum alloy. The concentrations of B_4C and 1100 aluminum, as well as the thickness and size of the plates, were changed, and the fuel rod configuration was adapted to ensure that the assembly would be critical in each case studied. A total of 10 critical configurations with a neutron absorber plate inserted are described in this report. No results of high-quality integral experiments involving neutron absorbers made with B_4C and 1100 aluminum plates are currently publicly available. Sensitivity to the neutron absorber plate material definition, isotopes, and cross sections of specific regions and configurations are also analyzed. The study results indicate that these experiments are achievable with sufficiently low uncertainties and minimal modification to the assembly. The experimental uncertainty can be further decreased with an additional characterization of the plates by x-ray computerized tomography or neutron radiography methods.

1. INTRODUCTION

The set of these experiments aims to produce additional critical benchmark data from the Sandia Pulsed Reactor Facility/Critical Experiments (SPRF/CX) apparatus at Sandia National Laboratories (SNL) using 7uPCX low-enriched uranium fuel (6.90%). These experiments aim to add Boralcan, a commercially available neutron absorber material, to the assembly and update the fuel rod configuration to reach criticality. The boron carbide (B_4C) neutron absorber plates are commonly used for spent fuel storage from commercial reactors, meaning knowing more about them is interesting for the whole nuclear fuel cycle. These plates made from B_4C dispersed in 1100 aluminum alloy are distinct from previous absorbers consisting of bulk B_4C plates clad in aluminum, which suffered from swelling. 1100 aluminum alloy is commonly used in applications requiring the highest proportion of aluminum possible, containing a minimum of 99% of aluminum. The use of the Boralcan plates in an integral experiment at the SPRF/CX will provide several benefits to the community. One of the benefits from these measurements will be the ability to probe the quality of the underlying nuclear data library specifically for B, C, and Al as well as the interaction of these nuclei with fissile actinides such uranium for a low-enriched configuration. Being for these experiments the fission events induced predominantly by thermal neutrons, the measured data will provide an integral metric of the interplay between a slowly varying cross section typical of light nuclei in this neutron energy region and the thermal constants together with first resonances typical of heavy fissile actinides. The nuclear data performance will be tested in terms of reactivity coefficients calculated by radiation transport criticality codes simulating the experiment in its geometry and materials as low-enriched uranium in water and neutron absorber plates made of B_4C and 1100 aluminum. Another benefit is to verify the uniformity of B_4C particles among the metallic matrix plate in an integral experiment. In criticality safety studies of spent fuel casks, the neutron absorbers are always modeled as a homogeneous aluminum alloy and B_4C material mixture. However, in real situations, the B_4C is a ceramic powder mixed with molten aluminum. Because the B_4C particles could form clusters, the B_4C may not be as uniformly distributed as in a homogeneous material. To test B_4C uniformity, calculations modeling the B_4C powder particles were performed and compared to the homogeneous mixture calculations. Conducting the experiment with the modeled plates ensures that both methods can be checked against reality, and the influence of the uniformity of the plates on the assembly criticality can be determined. Having more information about those plates could help industry members gain confidence in their modeling method and the use of this type of neutron absorber material. It would also help validate k_{eff} calculations and potentially justify relaxation of the boron loading credit limits in the Nuclear Regulatory commission Standard Review Plan for dry cask storage [1].

Results from experiments involving B_4C neutron absorbers can be found in the *International Handbook of Evaluated Criticality Safety Benchmark Experiments* (ICSBEP Handbook) [2] as the experiments performed in TRACY [3]. However, none of the experiments involve Boralcan, the most recent product developed by Rio Tinto that has been used in nuclear installations since approximately 2010 [4]. Also, most of the available benchmarks involve B_4C rods, and the Boralcan used in this study is in a thin plate shape. Furthermore, some of the available experiments are dated, so a high uncertainty regarding the materials or dimensions of various elements is possible. The SPRF/CX facility using the 7uPCX fuel rods is exceptionally well characterized, and the experimental uncertainty is minimized. This is proven by several previously published benchmarks in the ICSBEP Handbook as LEU-COMP-THERM-78 (LCT-78) [5] and the forthcoming LCT-102 [6]. Other efforts are ongoing to design new experiments, such as IER-304 [7] and IER-441 [8], in different steps of the CEdT integral experiment request process [9]. Therefore, adding these B_4C experiments to the ICSBEP Handbook [2] would greatly benefit the community.

Ten critical configurations are described in this report, each with a different neutron absorber plate inserted in its center or a different lattice configuration. The starting rod configuration of the assembly is

based on the IER-304 CED-2 report [7], case 9 of which shows a critical configuration using the 7uPCX fuel rods, with six central horizontal rows of fuel rods removed and replaced with water. In the first nine configurations described in this report, the neutron absorber plates are inserted in this central water channel. Additional fuel rods are added to the lattice's outer region or to the central channel to achieve criticality. In the tenth and last configuration described, the central channel is changed to a circular shape, which is similar to an experiment currently being designed with a central test region [8]. Rods are also added to achieve criticality. Using these ten different configurations makes it possible to test a wide range of B_4C concentrations, plate dimensions, neutron spectra, and energy corresponding to the average lethargy of neutrons causing fission (EALF).

This report includes several calculations required for the conceptual design or CED-1, the first step of the critical experiment design process defined by the Nuclear Criticality Safety Program NCSP [9]. All calculations are performed with SCALE 6.3.0/KENO V.a using the Evaluated Nuclear Data File (ENDF)/B-VII.1 continuous energy cross section library, and all results are given for a statistical calculation uncertainty of 10 pcm unless noted in the text. It is proposed that these experiments be performed with existing 7uPCX fuel rods at SNL. Nearly all physical components of the systems are kept the same as that documented in previously created benchmarks at the SPRF/CX critical assembly as LCT-78 [5], including the fuel rods, grid/pitch, detectors, assembly, dump tanks, and all other parts. Figure 1 presents an overview of the assembly from LCT-78 [5] loaded with the 7uPCX fuel rods.

Figure 2 shows the fuel rod layout in this assembly for case 9 of IER-304 CED-2 report [7], which is the s starting point of this study. The neutron absorber plates are placed vertically in the central channel, thus decreasing the assembly reactivity, and the fuel rod configuration is arranged to achieve criticality. A fuel layout of configuration 1, one of the new configurations proposed, is shown in Figure 3. These lattice structures are both near delayed critical when fully moderated and fully reflected by pure water regulated at 25 °C. The current setup still needs a means to ensure that the neutron absorber plates are immovable at the desired location in the assembly. A 3D cut view of the assembly with a neutron absorber plate inserted in its center is shown in Figure 4.
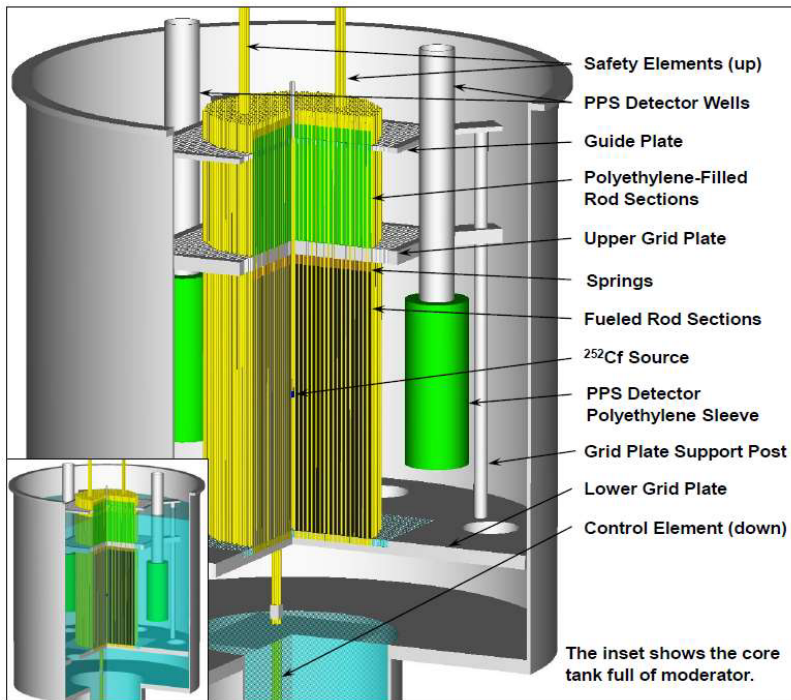
Figure 1. Experimental apparatus of the SPRF/CX from LEU-COMP-THERM-078 [5].

2
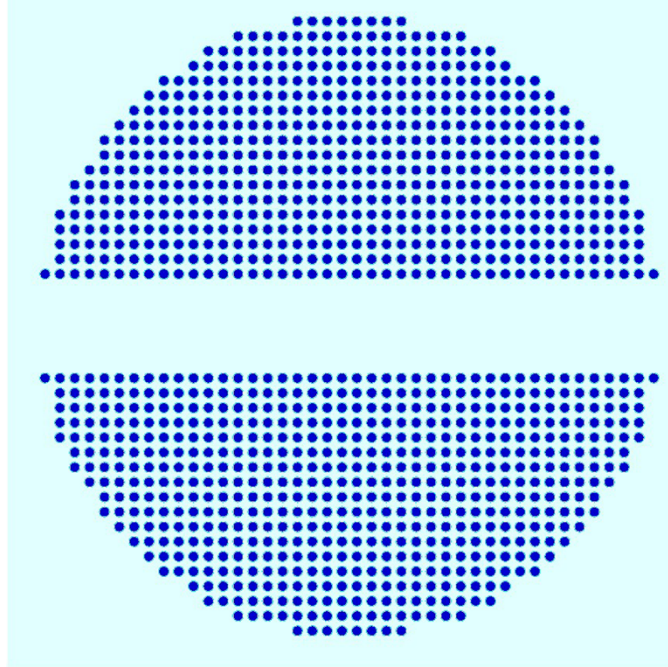
Figure 2. Fuel rod layout in Case 9 IER-304 CED-2 report [7].
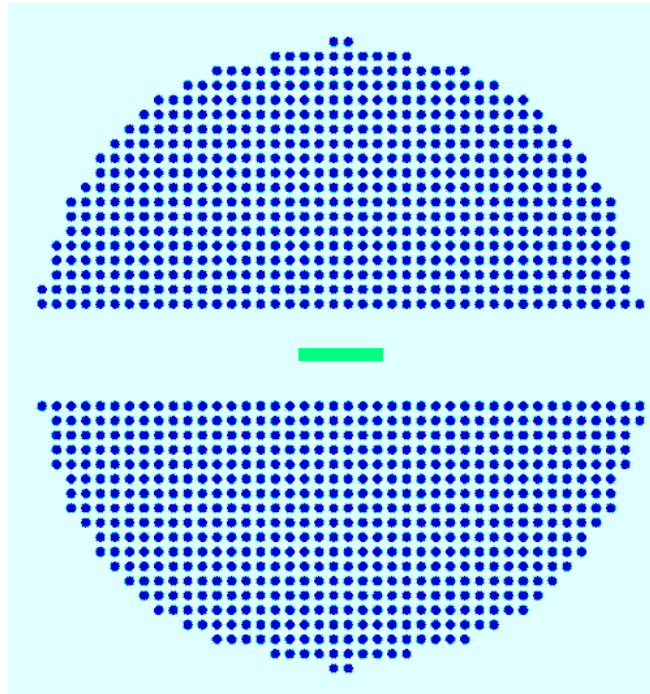
Figure 3. Fuel rod layout of proposed configuration 1. B$_4$C neutron absorber plate is shown in green.
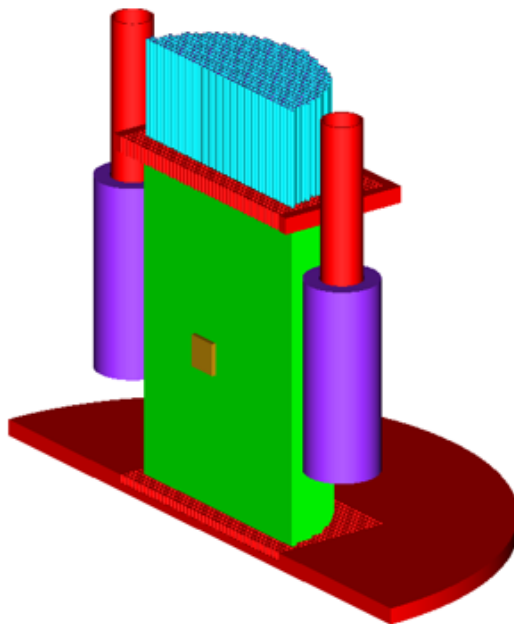
Figure 4. Example cutout view of the assembly with a neutron absorber plate in its center.

2. PROPOSED EXPERIMENT CONCEPT

The experiments described here as part of IER-554 are summarized in Table 1. The configurations all use the 7uPCX fuel rods with a pitch of 0.854964 cm. Basically, Boralcan plates of three different B_4C compositions and thicknesses are used, with three different width/length combinations for a total of 9 different plates and associated critical rod arrangements, plus an additional tenth configuration using the same plate as in configuration 1 and a different rod arrangement. By changing the layout of fuel rods to reach delayed critical, the use of these different combinations of Boralcan plate characteristics allows for the testing of a broader range of different parameters such as the EALF, neutron spectrum in the assembly, or k_{eff} material sensitivities. Configurations 1 through 3 use neutron absorber plates that measure 5 × 5 cm and a central water channel of 6 rows as shown in Figure 5. Configurations 4 through 6 use neutron absorber plates measuring 10 × 10 cm and a central water channel of 4 rows as shown in Figure 6. Configurations 7 through 9 use neutron absorber plates measuring 20 × 20 cm and a central water channel of 2 rows as shown in Figure 7. The tenth configuration uses the same plate as that used in configuration 1, with a circular water hole in the center of the assembly instead of a horizontal channel, as shown in Figure 8. During the approach to critical, the central channel or circular region should not be modified, and the rods should only be added to the outer locations of the array. In the ten critical configurations described, the neutron absorber plates are centralized in the assembly with the thin face perpendicular to the floor. For each of the ten critical configurations, additional calculations were performed, adding more depth to the information provided. A first set of additional calculations was performed by replacing the Boralcan plate replaced by a 1100 aluminum alloy plate of the same dimensions, and a second set by simply removing the plate from the assembly. Those experiments would help showing what is the impact of the Boralcan plate separated from the water displacement effect, giving more information as a result. Additional critical configurations testing different parameters could be obtained by changing the plate's position, inducing different effects on the assembly neutron spectrum. It would also be possible to change other parameters, such as the size of the water channel for a given plate width, the fuel rods' pitch, or to use different fuel rods available at the SPRF, such as the Burnup Credit Critical Experiment (BUCCX), for a different UO_2 enrichment and different neutron energy spectrum.

4

Table 1. Configuration description.

Configuration number	Boralcan sample characteristics			Central water region description	Fuel rods number	EALF at 25 °C (eV)
	B₄C concentration (vol %)	Width × length (cm)	Thickness (cm)			
1	16	5 × 5	0.75	6 rows central water channel	1,178	0.230
2	23	5 × 5	0.30		1,170	0.229
3	17	5 × 5	0.17		1,164	0.229
4	16	10 × 10	0.75	4 rows central channel	1,198	0.250
5	23	10 × 10	0.30		1,174	0.248
6	17	10 × 10	0.17		1,144	0.244
7	16	20 × 20	0.75	2 rows central channel	1,280	0.286
8	23	20 × 20	0.30		1,232	0.281
9	17	20 × 20	0.17		1,182	0.278
10	16	5 × 5	0.75	Circular central water region	1,262	0.262
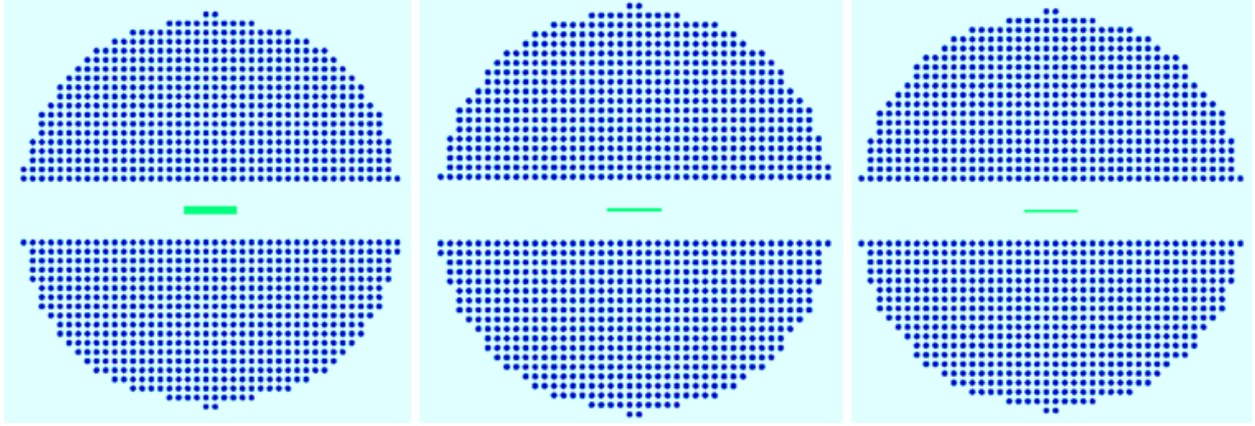
Figure 5. Configurations 1, 2, and 3.
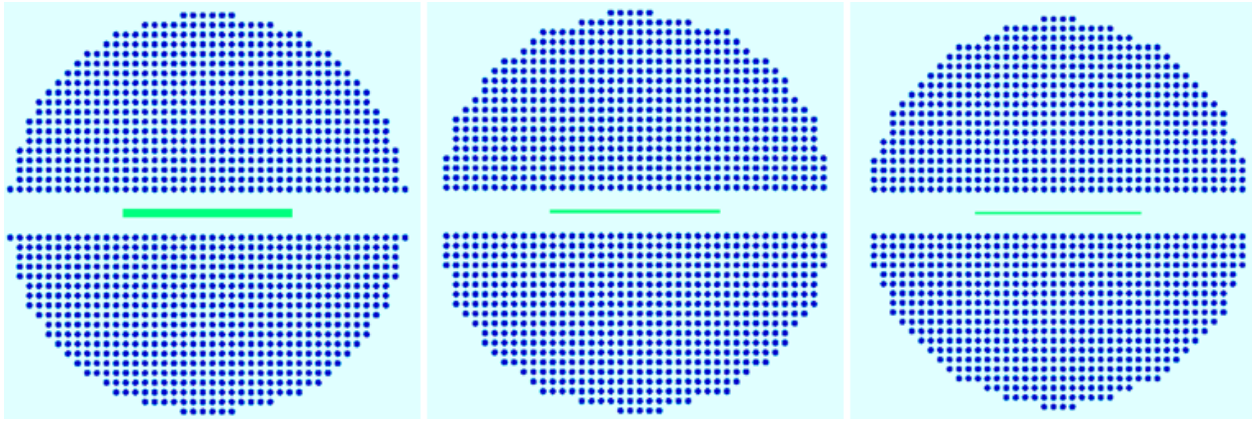
Figure 6. Configurations 4, 5, and 6.
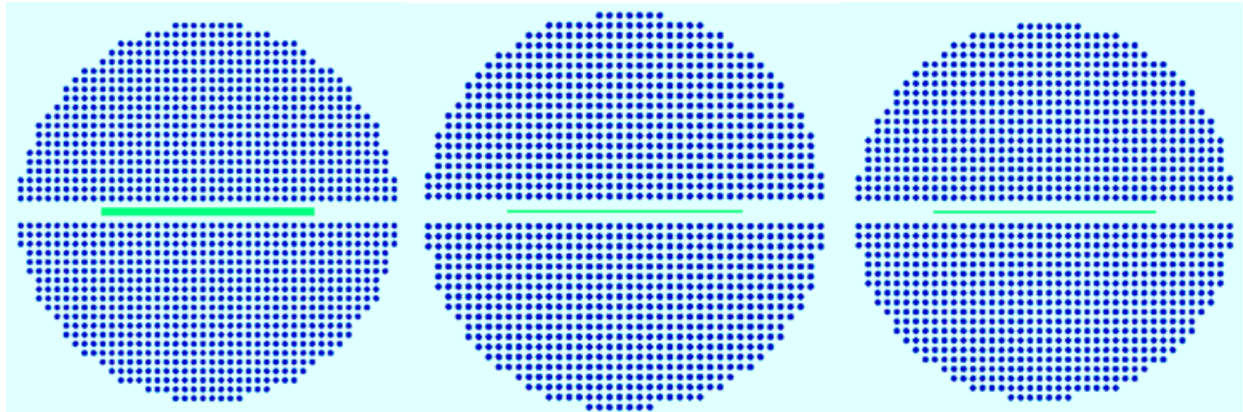
Figure 7. Configurations 7, 8, and 9.
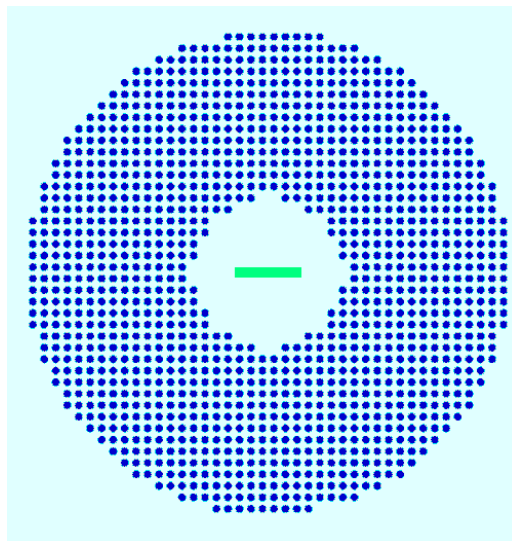
Figure 8. Configuration 10.

3. NEUTRON ABSORBER PLATES DESCRIPTION AND CHARACTERIZATION

3.1 NEUTRON ABSORBER PLATES PROCUREMENT

Several steps and companies are involved in creating the Boralcan neutron absorber final product using boron carbide as summarized in Figure 9. Rio Tinto is the manufacturer of the plates [10], and Manufacturing Sciences Corporation (MSC) is responsible to perform the final step: shaping and rolling the material before selling the product to nuclear installations [11]. MSC was contacted to procure Boralcan samples of small sizes. As of May 2022, samples from seven different B_4C concentrations and thicknesses were available to procure, as shown in Table 2. From these seven possibilities, three were selected to ensure the broadest range of parameters: plate 1 for its maximum thickness, plate 3 for its maximum B_4C concentration, and plate 4 for its minimal thickness of the seven possibilities. Plates 1–3 would require simple work to obtain the small samples, whereas plates 4–7 would require more work and could potentially cost more.

Figure 9. Overview of Boralcan product processing.

Table 2. Overview of available Boralcan sample products.

Sample number	Shape	Designation	Thickness (cm)	B_4C concentration (vol %)
1	Sheet form: easy treatment	W1100N.16B	0.75	16
2		W1100N.23B	0.20	23
3		W1100N.23B	0.30	23
4	Finished product form: more complex treatment	W1100N.17B	0.17	17
5		W1100N.17B	0.22	17
6		W1100N.19B	0.19	19
7		W1100N.21B	0.20	21

A verbal agreement was made with MSC to ensure that small samples from plates 1, 3, and 4 will be kept aside for the next few years for this experiment. MSC provided an informative budgetary quote for the procurement of several samples, as shown in section 8. MSC also provided various example documents characterizing each batch of products they receive from UK Abrasive and Rio Tinto, and excerpts are shown in Figure 10, Figure 11, and Figure 12 [12]. The same documents will be obtained for each plate procured from MSC. Capital information is obtained from these documents:

- B_4C Certificate of Conformance: measured boron and ^{10}B concentration, average measured B_4C powder particles size (Figure 10)
- Boralcan Chemical Analysis Certificate: 1100 aluminum material composition (Figure 11)
- Boralcan Metallographic report: overview of B_4C particles' uniformity in the finished Al-B_4C metal matrix product (Figure 12)

ISO 9001:2008#: 10893
DATE:
TO:
FROM:
RE: *CERTIFICATE OF CONFORMANCE (10 CFR PART 50 APPENDIX B,*
10 CFR PART 21),UK Abrasives
Q.A.Manual(Rev.5,06/29/11)

Rio Tinto Certificate
Customer Name: Alcan Inc.
Customer Purchase Order
Product: Boron Carbide F320 REV. 02

Parameters	Alcan Inc. Standard	UK lot plant
Total Boron%	76.0%min	78.43%
Total Carbon%	20.0%min	21.53%
B10 isotope	19.9± 0.3 Atom% min	20.0% Atom% (18.5 weight%)

NUCLEAR GRADE BORON CARBIDE FINISHED PRODUCT

Coulter Multisizer 3:

Lot#	3%	50%	94%
F320 Standard Sedigraph	49micron max	27.7-30.7micron	16.5 micron min
F320 Standard Multisizer	50.0 micron max	28.0-32.0 micron	16.9 micron
	45.17	31.37	20.57

Figure 10. Excerpt of example B_4C powder Certificate of Conformance [12].

Rio Tinto Dubuc Works	Chemical Analysis Certificate	NO:
		Date:
		Page: 1 of 1

| Customer | Manufacturing Sciences Corporation | Heat #: | |
| P.O. # : | (Attachments A, B ,C) | Material: | Boron MMC W1100N.21B V% |

CERTIFICAT D`ANALYSE / CERTIFICATE OF ANALYSIS

No. Coulée / Cast ID	Produit/ Product	Alliage (AA)/ Alloy (AA)	Date de l'analyse/ Date of analysis
	W1100N.21B	10116 (W1100N.21B)	

COMPOSITION CHIMIQUE/ CHEMICAL COMPOSITION

Elément/ Element	% Masse/ % Weight	% Vol.céramique/ Ceramic Vol. Fraction%
Si	0.15	
Fe	0.28	
Cu	0.11	
Mn	< 0.01	
Mg	< 0.01	
Zn	< 0.01	
Traces	0.02	
Fe+Si	0.43	

Les analyses ci-dessus sont conformes aux spécifications. Above analysis are certified conform to specifications.
* Tous les alliages de fonderie Duralcan sont modifiés au Strontium. All Duralcan foundry alloys are Strontium modified.

Figure 11. Excerpt of example Boralcan Chemical Analysis Certificate [12].

Pictures of a representative sample
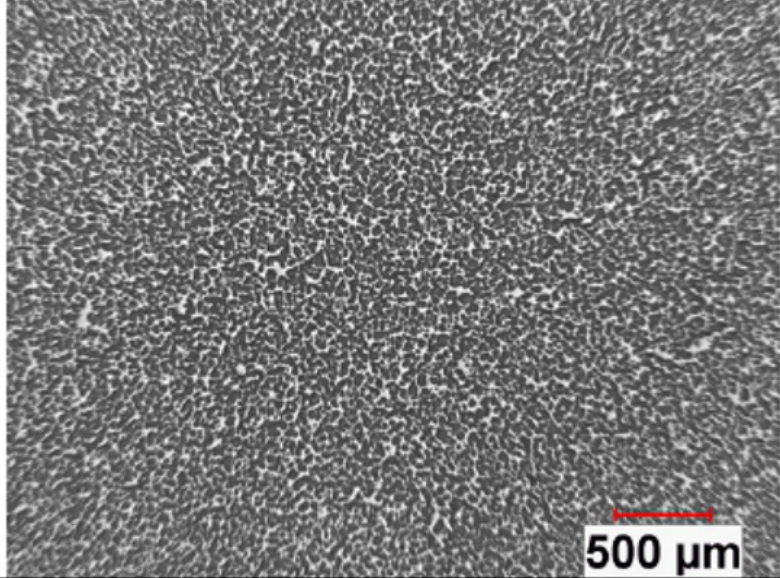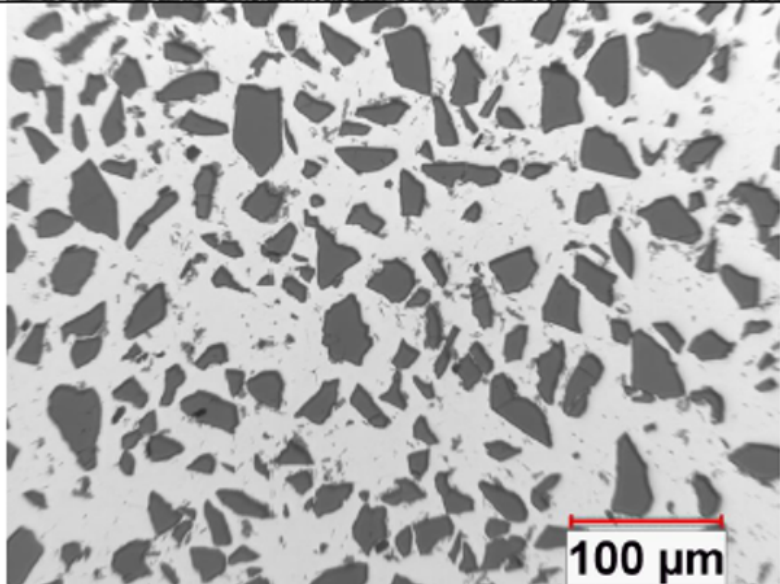
Figure 12. Excerpt of example Boralcan Metallographic Analysis Certificate [12].

3.2 PRELIMINARY STUDY OF THE INFLUENCE OF THE UNIFORMITY OF B_4C PARTICLES IN BORALCAN

Regardless of the valuable information shown in the previous section, the exact material composition of the plates and the uniformity of the B_4C powder concentration in the plate can still be questioned. For example, the uniformity of B_4C particles in the plate could be modified when MSC performs the rolling of the Boralcan products. To reduce uncertainty in the plates' characteristics, another plate characterization will be performed by ORNL when the plates are procured. According to the documents previously shown, the B_4C particles to be resolved by the imaging system are estimated to be between 10 and 100 μm. After internal discussions [13], several possibilities are considered. The most promising possibility is imaging by x-ray method with a computerized tomography (CT) system from the Materials Science and Technology Division (MSTD) at ORNL, a Zeiss Versa 510 [14] shown in Figure 13. This system can achieve 700-nanometer spatial resolution and 70-nanometer voxels in a 3D picture. According to Philip Bingham [13], even if the B_4C and aluminum alloys have a similar density (around 2.52 g/cm^3 and 2.71 g/cm^3, respectively), the cross section with x-rays of 50KV are different enough to have a factor 2 in contrast between B_4C, probably enough for the present application. Other possibilities could be Neutron Radiography at the Spallation Neutron Source (SNS), the High Flux Isotope Reactor (HIFR) at ORNL, or the Annular Core Research Reactor (ACRR) at SNL. According to Philip Bingham, the small size of the B_4C particles could be a challenge for neutron radiography. Performing the imaging at ORNL would be beneficial for a few reasons. It would be free as the only cost would be labor, and the x-ray imaging would not require a proposal cycle. Overall, it would just be simpler. To evaluate potential differences between each sample because of potential B_4C particle clusters, it is proposed to procure two or three identical samples for each of the nine plates described in Section 2, for a total of 27 samples. If differences are found between the three plates that are theoretically the same, then it would be useful to model those differences with KENO to see the influence on k_{eff}. Similarly, using those three plates in the actual experiment at the SPRF would show the significance of the differences for assembly criticality. Additionally, the neutron absorber plates should be characterized by mass spectrometry to obtain a more precise density, elemental/isotopic composition, and associated uncertainties.

Figure 13. Zeiss versa 510 X-ray CT system used at ORNL MSTD [14].

In the design calculations performed with SCALE 6.3.0/KENO V.a, the neutron absorber plates are modeled as a single homogeneous material. For example, the modeled composition of plate 1 as used in configurations 1, 4, 7, and 10 is shown in Table 3, as estimated from the information provided in the material characterization documents obtained from MSC. The natural isotopic abundance given by SCALE is used for the all the elements but Boron. In reality, the B_4C particles have a finite size, and if the uniformity of the B_4C particle concentration is not adequate, then a different influence on k_{eff} could be obtained, depending on the sample used for the same theoretical and measured material composition. Plate 1 was modeled with individual B_4C particles to investigate this potential issue, as shown in Figure 14. In this study, the B_4C particles are considered as spheres of the same size and pitch. Using the example B_4C certificate of conformance and the metallographic analysis certificates previously shown, two sizes of B_4C particles measuring 30 and 100 μm in diameter were selected to be modeled. To conserve a total B_4C mass equivalent to the homogeneous mixture model, a spacing between the B_4C spheres was derived, giving a total number of B_4C spheres in the plate for each modeled B_4C sphere size and each plate size, as shown in

Table 4 for the two B$_4$C sphere sizes and two critical configurations (configuration 1 with a 5 × 5 × 0.75 cm plate and configuration 7 with a 20 × 20 × 0.75 cm plate). The comparison of calculated k$_{eff}$ obtained between a homogeneous material mixture and the explicitly modeled B$_4$C spheres for different possibilities is shown in Table 5. From those results, it can be concluded that the size of the B$_4$C particles has practically no influence on k$_{eff}$ as long as the total B$_4$C mass is conserved. Modeling the B$_4$C particles individually or as a homogeneous material may be statistically insignificant (within a few pcm). Based on these encouraging preliminary results, it appears that using a homogeneous material mixture and explicitly modeling the B$_4$C particles as uniformly spaced spheres of the same size give the same results. In the final design calculations (CED-2), more tests can be added to determine the influence of explicitly modeling the B$_4$C particles on k$_{eff}$. For example, the B$_4$C could be of various shapes other than spheres, their positions and sizes could be randomly sampled in the plate, and the plate could be rotated inside the assembly, always keeping the same B$_4$C and aluminum alloy total masses. The sensitivity of k$_{eff}$ to these different tests can be obtained, and the correctness of these hypotheses can be checked by comparing the results to the actual experiments. For example, flipping the plates upside down in the experiments could reveal potential B$_4$C non-uniformity in the plate and the assembly criticality could be different. In a similar fashion, different plates of the theoretically same material composition can be interchanged.

Table 3. Modeled material composition of plate 1 used in configurations 1, 4, 7, and 10.

Boralcan plate 1 (estimated density 2.71763 g/cm^3)				
1100 aluminum mass fraction (83.1 wt%)		**B$_4$C mass fraction (14.9 wt%)**		**Titanium mass fraction (2 wt%)**
Magnesium	0.005	Carbon	22.69	
Aluminum	99.445	Boron	77.31	
Silicon	0.15	**Boron isotopes mass fraction (wt %)**		
Manganese	0.005	Boron-10	18.60	
Iron	0.28	Boron-11	81.40	
Copper	0.11			
Zinc	0.005			
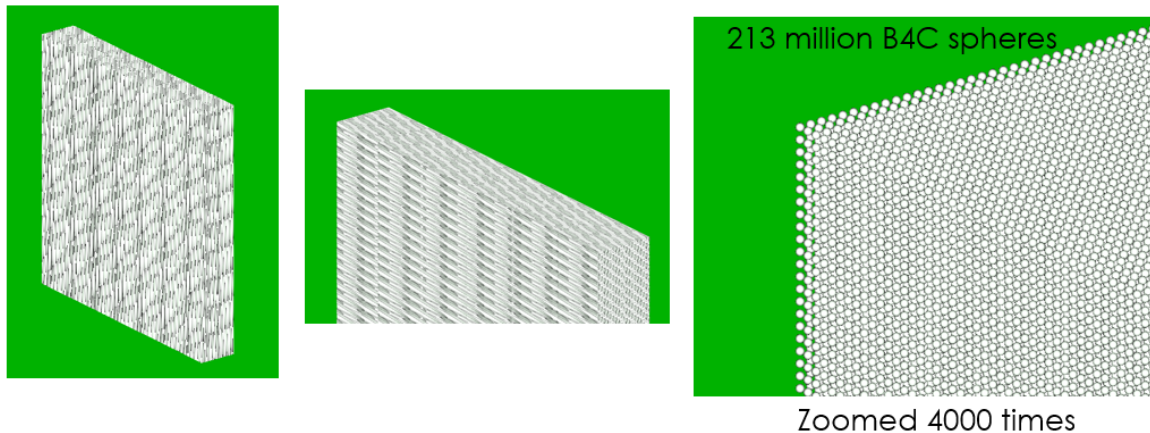
Figure 14. Plate 1 with B$_4$C particles individually modeled, zoomed in from left to right.

13

Table 4. Overview of Boralcan plates with individually modeled
B_4C particle characteristics from plate 1 material definition.

Trial number	Plate dimensions (width × length × thickness in cm)	Estimated B_4C mass (g)	B_4C sphere diameter (μm)	Number of B_4C spheres required (millions)	Corresponding spacing between each B_4C sphere (μm)
1	5 × 5 × 0.75	7.59	100	6	47.00
2	5 × 5 × 0.75	7.59	30	213	14.32
3	20 × 20 × 0.75	121.49	100	92	47.00
4	20 × 20 × 0.75	121.49	30	3410	14.32

Table 5. Influence on k_{eff} of modeling Boralcan as a homogeneous material
or as individually B_4C particles spheres of the same diameter and uniformly spaced.

Modeling method	Plate dimensions (width × length × thickness in cm)	Equivalent critical configuration number from Table 1	B_4C sphere diameter (μm)	k_{eff} (sig=0.00010)
Homogeneous	5 × 5 × 0.75	Configuration 1	N/A	1.00006
Individually modeled B_4C particles	5 × 5 × 0.75	Configuration 1	100	0.99993
Individually modeled B_4C particles	5 × 5 × 0.75	Configuration 1	30	0.99988
Homogeneous	20 × 20 × 0.75	Configuration 7	N/A	1.00023
Individually modeled B_4C particles	20 × 20 × 0.75	Configuration 7	100	1.00031
Individually modeled B_4C particles	20 × 20 × 0.75	Configuration 7	30	1.00034

3.3   PLATES SUPPORTS PRELIMINARY STUDY

The plates should be held and remain immovable in the assembly during the experiments. To facilitate the insertion of the plates in the system with a minimal effect on k_{eff}, a rough system of slotted aluminum rod holders was modeled in KENO V.a as shown in Figure 15. In this example, the largest plate (20 × 20 × 0.75 cm) is supported by 16 slotted aluminum rods. If the guide plate and upper grid plates of the assembly were removed, then the absorber plates could be inserted and guided using the fuel rod inserts in the lower grid plate. Calculations using these slotted aluminum rods showed a negligible effect on k_{eff} compared to not having any support for the plate (the k_{eff} difference was within the calculation uncertainty of 30 pcm), even when using a greater number of them, as shown in Figure 15. Using a similar system to hold the absorber plate in the experiments would be beneficial because of its simplicity, low cost, and no influence on the assembly criticality. Despite those good points, the system shown could prove to be impractical as it would be difficult for the slotted aluminum rods to all be inserted in the top grid plate. Furthermore, the plate support system should be as safe as possible as it could be a safety hazard. In the next phase CED-2, an updated design for the plate supports will be given, and the final mechanical design for all new hardware necessary for the experiments will be done by SNL in the CED-3a phase.
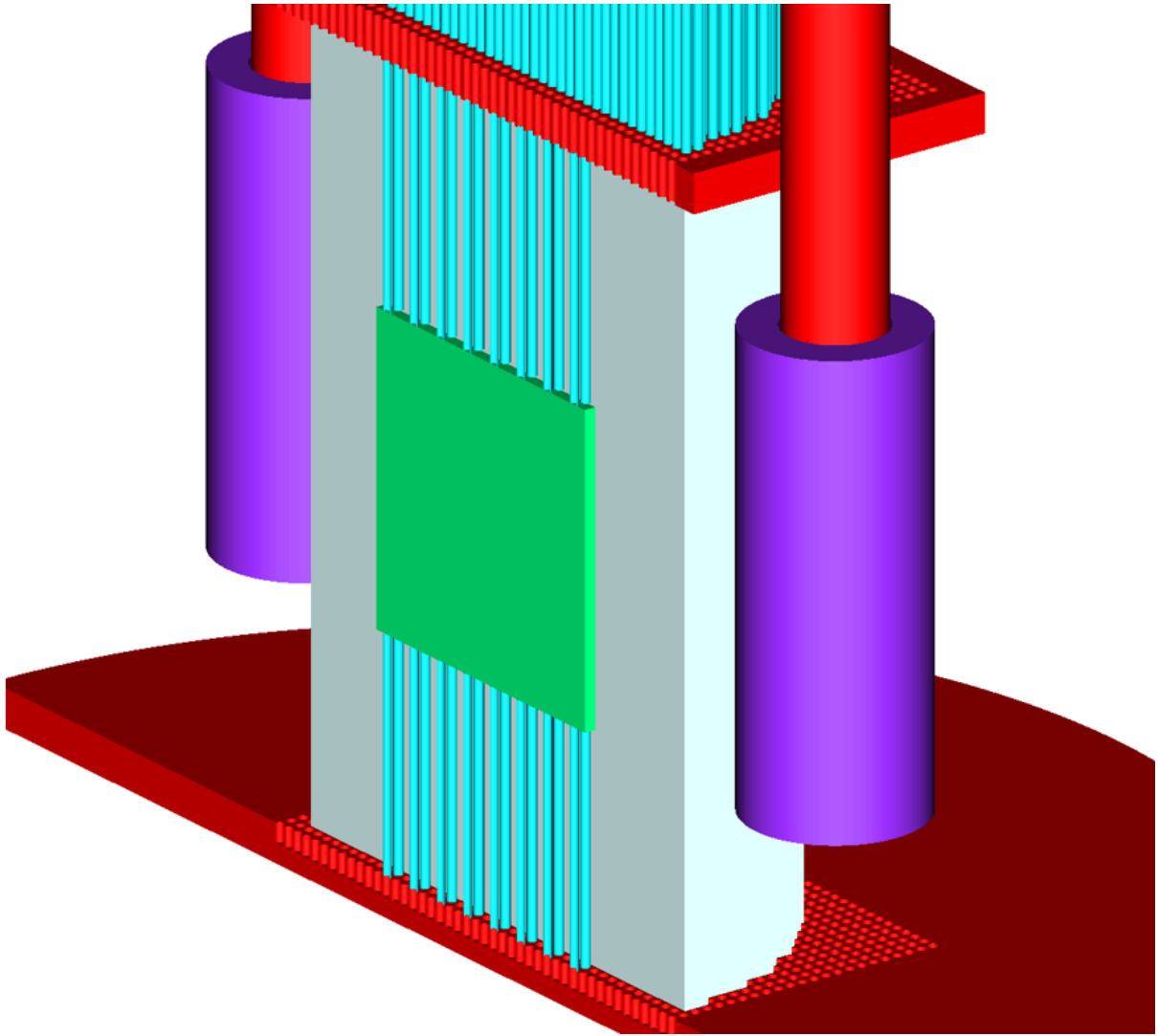
Figure 15. Example of potential plate support by slotted aluminum rods.

4. DETAILED DESCRIPTION OF THE PROPOSED EXPERIMENTS

In this section, the ten critical configurations are described in more detail. For each configuration, the following information is given:

- Table summarizing the primary information about the configuration (plate characteristics, k_{eff} with and without the neutron absorber plate, k_{eff} with the neutron absorber plate replaced by an aluminum plate)
- Rod layout with the array visible to facilitate rod placement
- Fission map

An overview of the ten configurations' characteristics is given in Table 6. This information is similar to that given in Table 1, but with k_{eff} calculation results and some other parameters. For configuration 10, the water channel is circular, so the "Water channel width (cm)" value given in the table corresponds to the approximate water channel diameter instead. The influence of the insertion of the Boralcan plates in the assembly is observed, with a loss of about 500–600 pcm with the insertion of the 5 × 5 cm plate, 3,300–4,100 pcm with the insertion of the 10 × 10 plate, and 4,600–6,100 pcm with the insertion of the 20 × 20 plate, depending on the plate's thickness and B_4C concentration. Replacing the neutron absorber plate with an aluminum plate significantly increases k_{eff} to be close to a configuration with no plate inserted.

Table 6. Overview of the ten critical configurations characteristics with k_{eff} calculation results.

| Configuration number | Boralcan sample characteristics | | | Fuel rods number | Water channel width (cm) | EALF at 25 °C (eV) | k_{eff} | k_{eff} without plate | k_{eff} with aluminum plate |
	B_4C concentration (vol %)	Width × length (cm)	Thickness (cm)						
1	16	5 × 5	0.75	1,178	5.13	0.230	1.00006	1.00685	1.00710
2	23	5 × 5	0.30	1,170	5.13	0.229	0.99983	1.00597	1.00620
3	17	5 × 5	0.17	1,164	5.13	0.229	0.99981	1.00498	1.00497
4	16	10 × 10	0.75	1,198	3.42	0.250	0.99981	1.04151	1.04065
5	23	10 × 10	0.30	1,174	3.42	0.248	0.99950	1.03740	1.03710
6	17	10 × 10	0.17	1,144	3.42	0.244	0.99997	1.03299	1.03278
7	16	20 × 20	0.75	1,280	1.71	0.286	1.00023	1.06171	1.05479
8	23	20 × 20	0.30	1,232	1.71	0.281	0.99995	1.05462	1.05194
9	17	20 × 20	0.17	1,182	1.71	0.278	0.99987	1.04656	1.04496
10	16	5 × 5	0.75	1,262	11.97	0.262	0.99992	1.00526	1.00563

4.1 CONFIGURATION 1

An overview of the configuration 1 characteristics is given in Table 7. The rod layout is given in Figure 16, and the fission map is given in Figure 17.

Table 7. Overview of configuration 1 characteristics.

Configuration 1: 6 rows central water channel and Plate 1 of 5 × 5 × 0.75 cm							
Boralcan sample characteristics			Fuel rods number	EALF at 25 °C (eV)	k_{eff}	k_{eff} without plate	k_{eff} with aluminum plate
B$_4$C concentration (vol %)	Width × length (cm)	Thickness (cm)					
16	5 × 5	0.75	1,178	0.230	1.00006	1.00685	1.00710
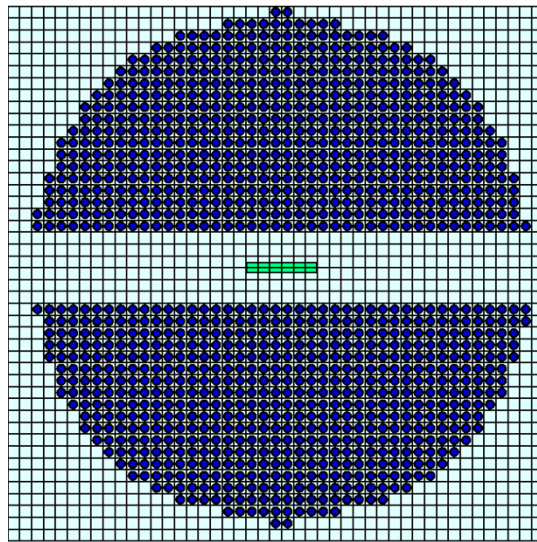
Figure 16. Configuration 1 rod layout.

Figure 17. Configuration 1 fission map, fissions neutrons per cm³ per source neutron.

4.2 CONFIGURATION 2

An overview of the configuration 2 characteristics is given in Table 8. The rod layout is given in Figure 18, and the fission map is given in Figure 19.

Table 8. Overview of configuration 2 characteristics.

Configuration 2: 6 rows central water channel and Plate 3 of 5 × 5 × 0.30 cm							
Boralcan sample characteristics			Fuel rods number	EALF at 25 °C (eV)	k_{eff}	k_{eff} without plate	k_{eff} with aluminum plate
B$_4$C concentration (vol %)	Width × length (cm)	Thickness (cm)					
23	5 × 5	0.30	1,170	0.229	0.99983	1.00597	1.00620
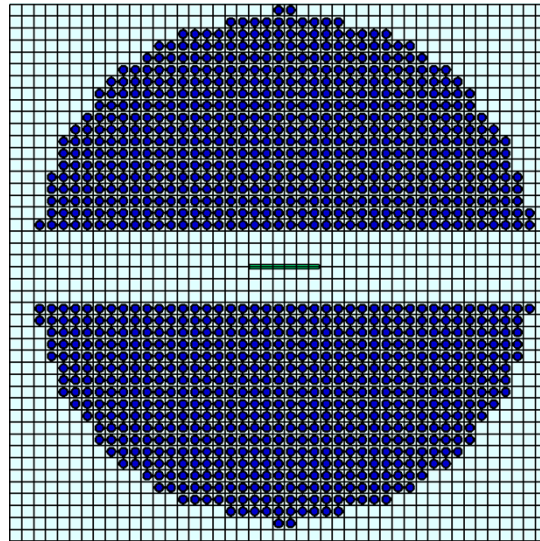
Figure 18. Configuration 2 rod layout.

Figure 19. Configuration 2 fission map, fissions neutrons per cm³ per source neutron.

19

4.3   CONFIGURATION 3

An overview of the configuration 3 characteristics is given in Table 9. The rod layout is given in Figure 20, and the fission map is given in Figure 21.

Table 9. Overview of configuration 3 characteristics.

Configuration 3: 6-row central water channel and Plate 4 of 5 × 5 × 0.17 cm							
Boralcan sample characteristics			Fuel rods number	EALF at 25 °C (eV)	k_{eff}	k_{eff} without plate	k_{eff} with aluminum plate
B_4C concentration (vol %)	Width × length (cm)	Thickness (cm)					
17	5 × 5	0.17	1,164	0.229	0.99981	1.00498	1.00497
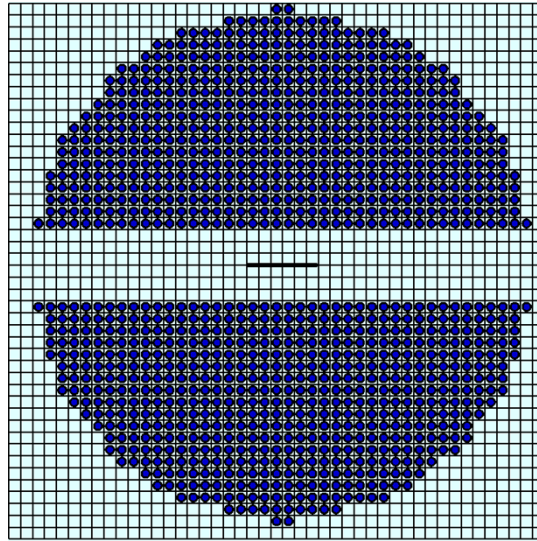
Figure 20. Configuration 3 rod layout.

Figure 21. Configuration 3 fission map, fissions neutrons per cm³ per source neutron.

20

4.4 CONFIGURATION 4

An overview of the configuration 4 characteristics is given in Table 10. The rod layout is given in Figure 22, and the fission map is given in Figure 23.

Table 10. Overview of configuration 4 characteristics.

Configuration 4: 4 rows central water channel and Plate 1 of 10 × 10 × 0.75 cm							
Boralcan sample characteristics			Fuel rods number	EALF at 25 °C (eV)	k_{eff}	k_{eff} without plate	k_{eff} with aluminum plate
B₄C concentration (vol %)	Width × length (cm)	Thickness (cm)					
16	10 × 10	0.75	1,198	0.250	0.99981	1.04151	1.04065
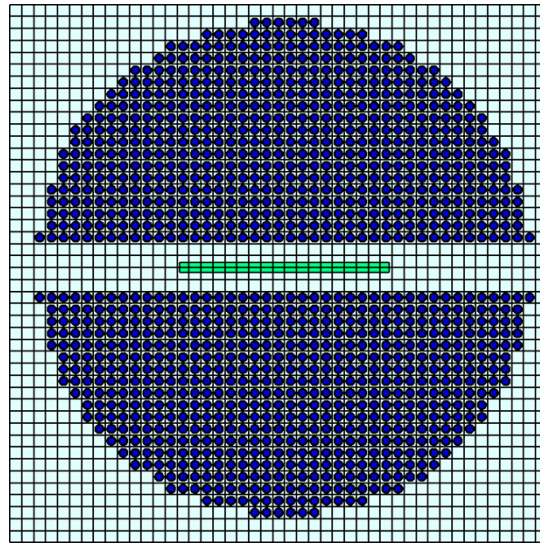
Figure 22. Configuration 4 rod layout.

Figure 23. Configuration 4 fission map, fissions neutrons per cm³ per source neutron.

4.5   CONFIGURATION 5

An overview of the configuration 5 characteristics is given in Table 11. The rod layout is given in Figure 24, and the fission map is given in Figure 25.

Table 11. Overview of configuration 5 characteristics.

| Configuration 5: 4 rows central water channel and Plate 3 of 10 × 10 × 0.30 cm							
Boralcan sample characteristics			Fuel rods number	EALF at 25 °C (eV)	k_{eff}	k_{eff} without plate	k_{eff} with aluminum plate
B₄C concentration (vol %)	Width × length (cm)	Thickness (cm)					
23	10 × 10	0.30	1,174	0.248	0.99950	1.03740	1.03710
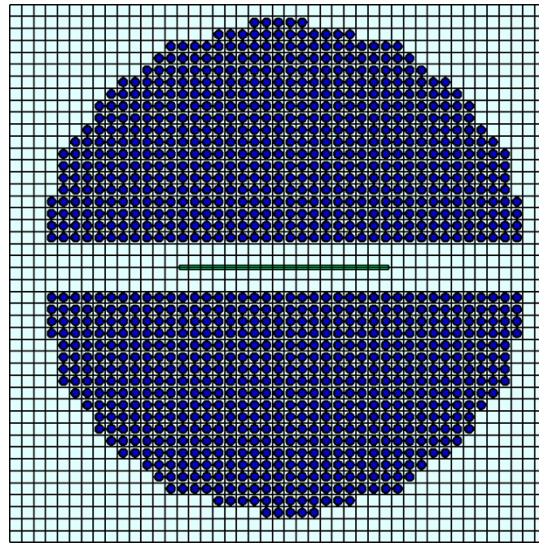
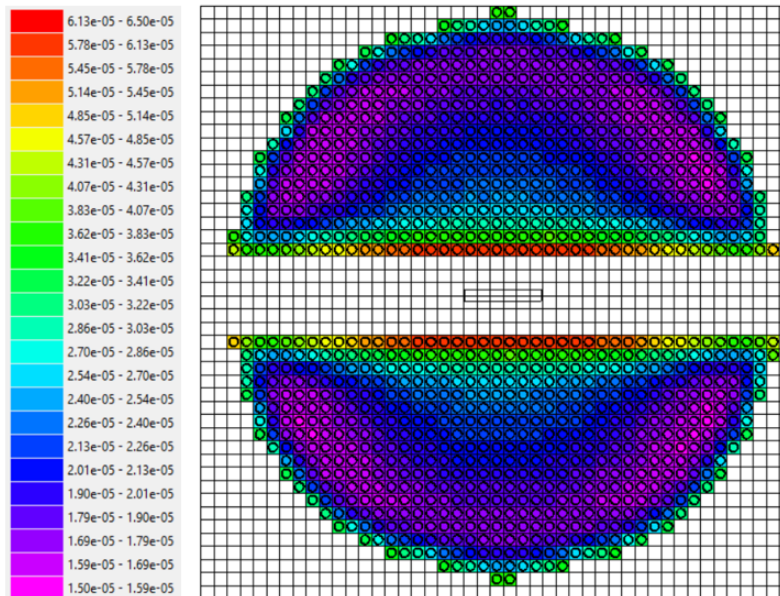**Figure 24. Configuration 5 rod layout.**

Figure 25. Configuration 5 fission map, fissions neutrons per cm³ per source neutron.

4.6 CONFIGURATION 6

An overview of the configuration 6 characteristics is given in Table 12. The rod layout is given in Figure 26, and the fission map is given in Figure 27.

Table 12. Overview of configuration 6 characteristics.

| Configuration 6: 4 rows central water channel and Plate 4 of 10 × 10 × 0.17 cm							
Boralcan sample characteristics			Fuel rods number	EALF at 25 °C (eV)	k_{eff}	k_{eff} without plate	k_{eff} with aluminum plate
B₄C concentration (vol %)	Width × length (cm)	Thickness (cm)					
17	10 × 10	0.17	1,144	0.244	0.99997	1.03299	1.03278
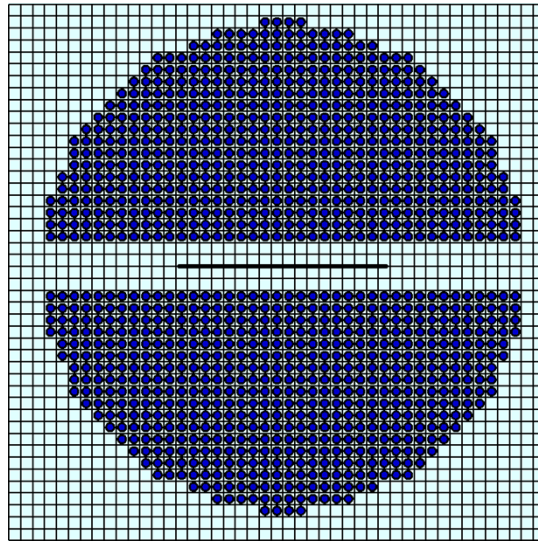
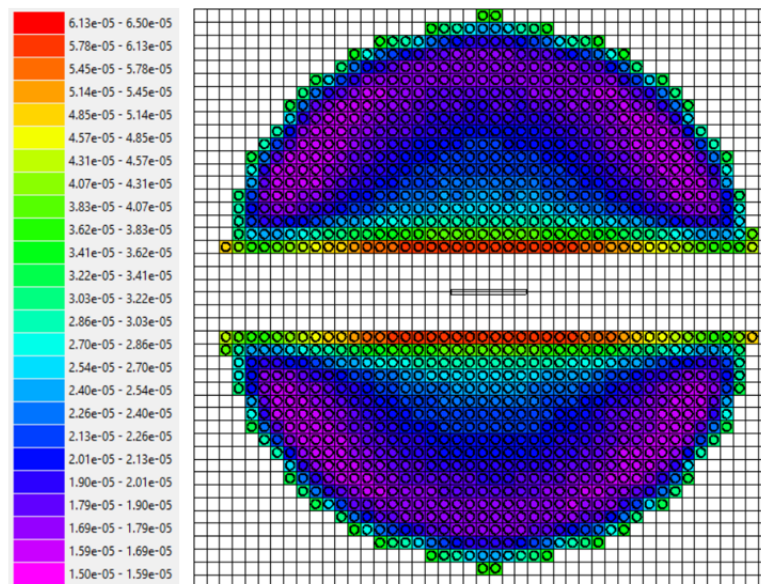**Figure 26. Configuration 6 rod layout.**
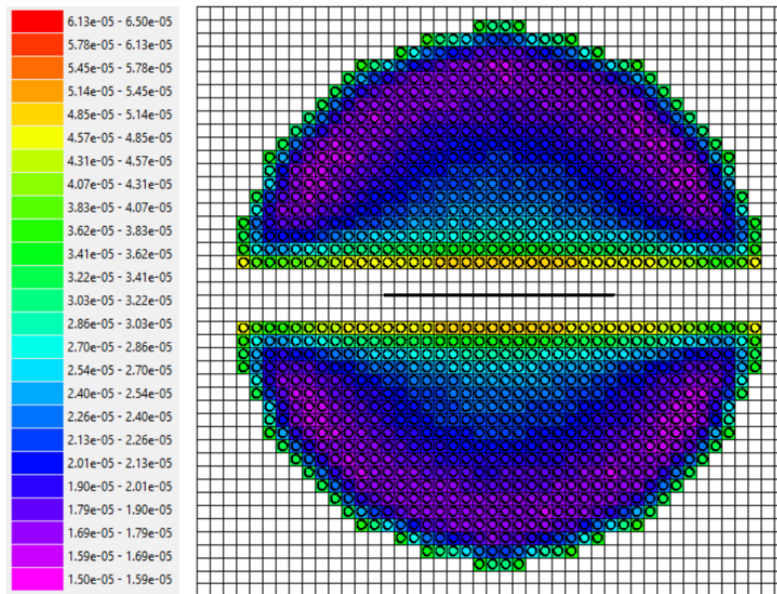
Figure 27. Configuration 6 fission map, fissions neutrons per cm³ per source neutron.

23

4.7 CONFIGURATION 7

An overview of the configuration 7 characteristics is given in Table 13. The rod layout is given in Figure 28, and the fission map is given in Figure 29.

Table 13. Overview of configuration 7 characteristics.

| Configuration 7: 2 rows central water channel and Plate 1 of 20 × 20 × 0.75 cm							
Boralcan sample characteristics			Fuel rods number	EALF at 25 °C (eV)	k_{eff}	k_{eff} without plate	k_{eff} with aluminum plate
B₄C concentration (vol %)	Width × length (cm)	Thickness (cm)					
16	20 × 20	0.75	1,280	0.286	1.00023	1.06171	1.05479
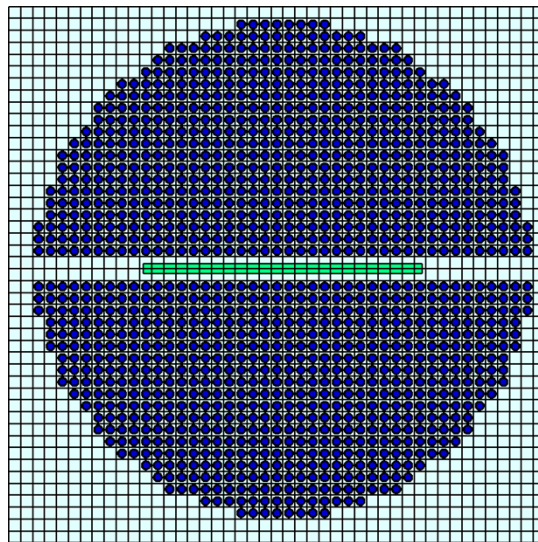
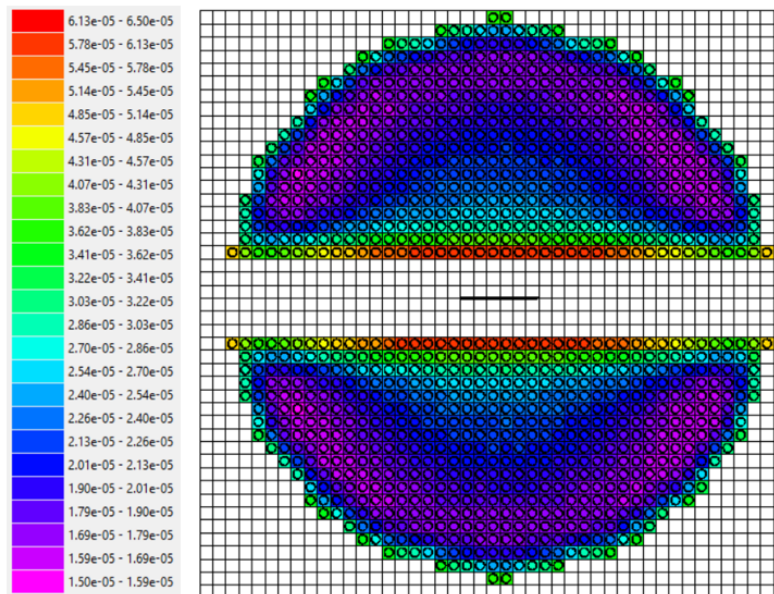**Figure 28. Configuration 7 rod layout.**
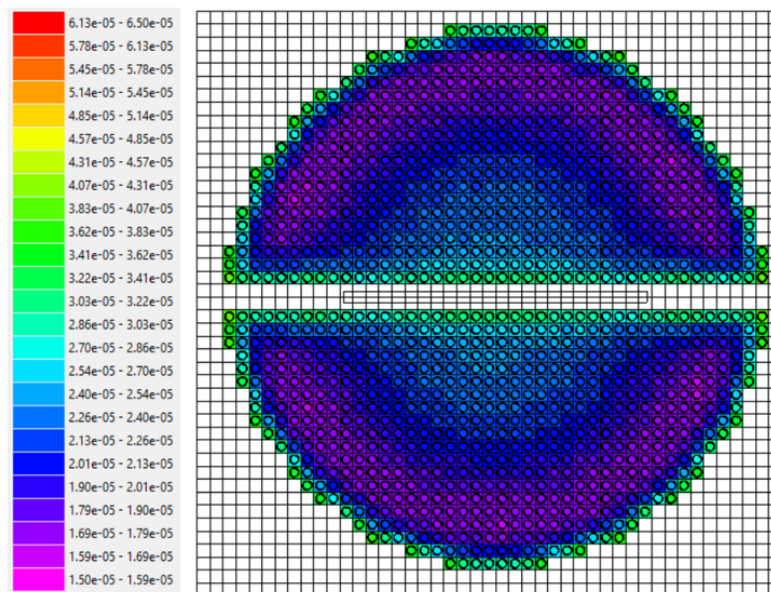
Figure 29. Configuration 7 fission map, fissions neutrons per cm³ per source neutron.

4.8   CONFIGURATION 8

An overview of the configuration 8 characteristics is given in Table 14. The rod layout is given in Figure 30, and the fission map is given in Figure 31.

Table 14. Overview of configuration 8 characteristics.

| Configuration 8: 2 rows central water channel and Plate 3 of 20 × 20 × 0.30 cm							
Boralcan sample characteristics			Fuel rods number	EALF at 25 °C (eV)	k_{eff}	k_{eff} without plate	k_{eff} with aluminum plate
B_4C concentration (vol %)	Width × length (cm)	Thickness (cm)					
23	20 × 20	0.30	1,232	0.281	0.99995	1.05462	1.05194
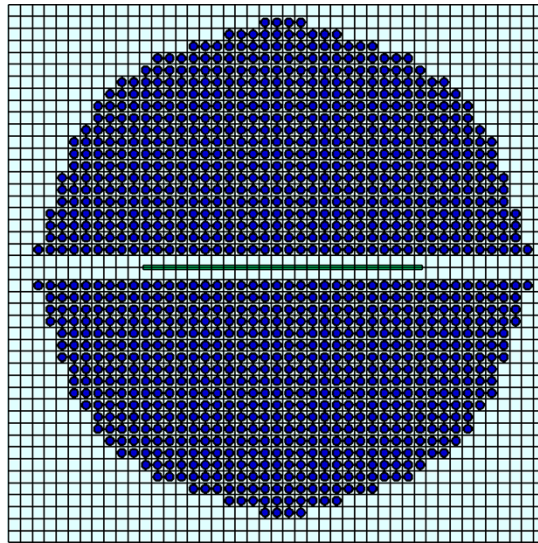
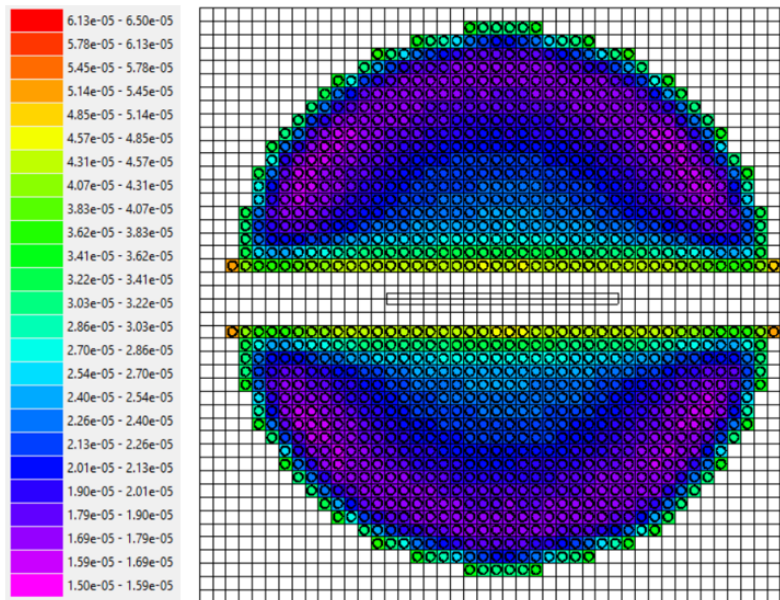**Figure 30. Configuration 8 rod layout.**
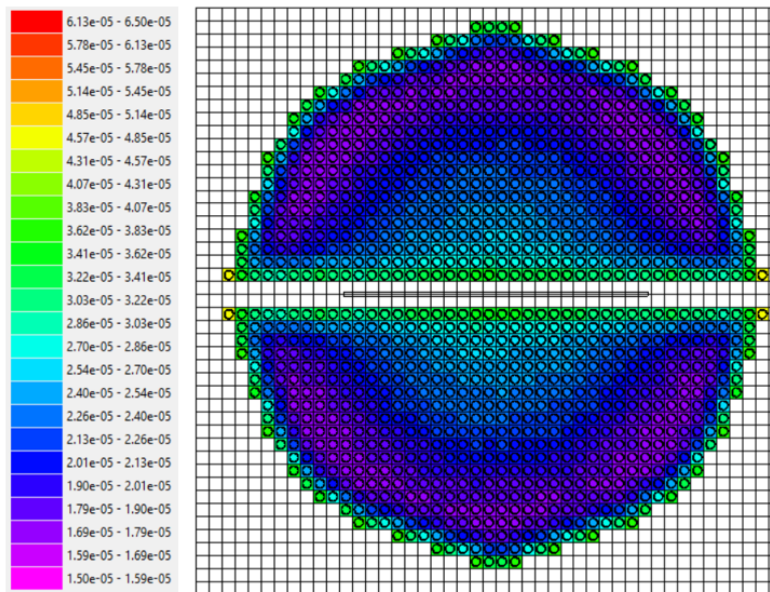
Figure 31. Configuration 8 fission map, fissions neutrons per cm³ per source neutron.

25

4.9   CONFIGURATION 9

An overview of the configuration 9 characteristics is given in Table 15. The rod layout is given in Figure 32, and the fission map is given in Figure 33.

Table 15. Overview of configuration 9 characteristics.

| Configuration 9: 2 rows central water channel and Plate 4 of 20 × 20 × 0.17 cm							
Boralcan sample characteristics			Fuel rods number	EALF at 25 °C (eV)	k_{eff}	k_{eff} without plate	k_{eff} with aluminum plate
B₄C concentration (vol %)	Width × length (cm)	Thickness (cm)					
17	20 × 20	0.17	1,182	0.278	0.99987	1.04656	1.04496

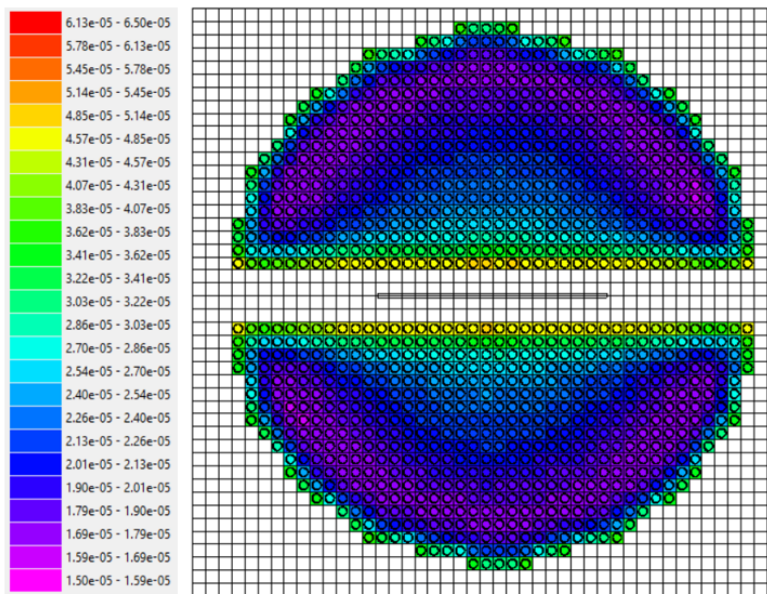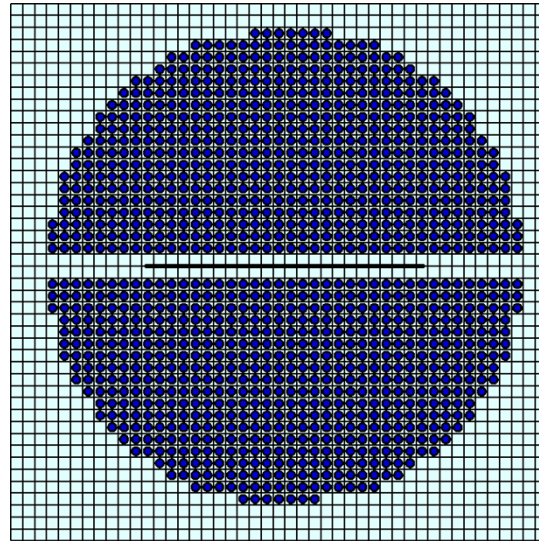**Figure 32. Configuration 9 rod layout.**
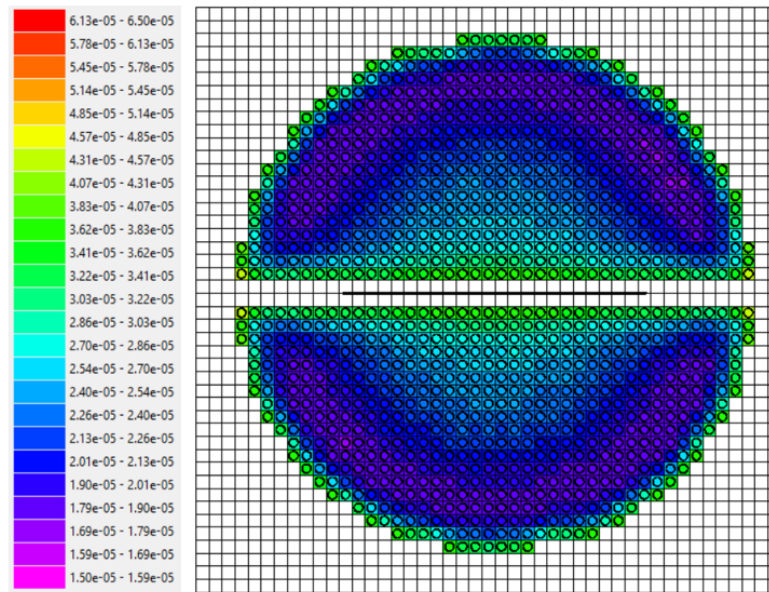
Figure 33. Configuration 9 fission map, fissions neutrons per cm³ per source neutron.

26

4.10 CONFIGURATION 10

An overview of the configuration 10 characteristics is given in Table 16. The rod layout is given in Figure 34, and the fission map is given in Figure 35.

Table 16. Overview of configuration 10 characteristics.

Configuration 10: Circular central water region and Plate 1 of 5 × 5 × 0.75 cm							
Boralcan sample characteristics			Fuel rods number	EALF at 25 °C (eV)	k_{eff}	k_{eff} without plate	k_{eff} with aluminum plate
B_4C concentration (vol %)	Width × length (cm)	Thickness (cm)					
16	5 × 5	0.75	1,262	0.262	0.99992	1.00526	1.00563
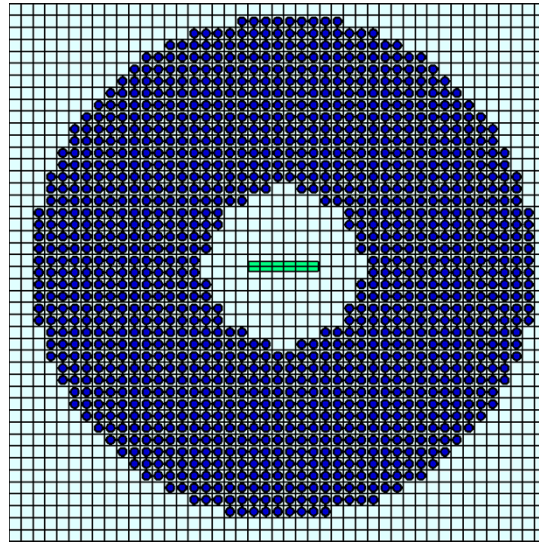
Figure 34. Configuration 10 rod layout.
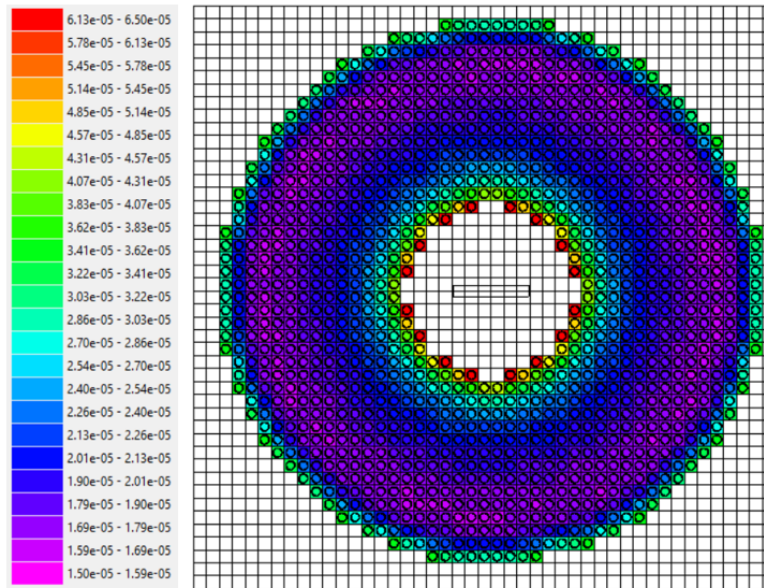
Figure 35. Configuration 10 fission map, fissions neutrons per cm^3 per source neutron.

5. SPECTRAL COMPARISONS

The neutron spectra calculated by KENO V.a in the fuel, moderator in a fuel pin cell, and reflector water are shown in **Error! Reference source not found.** for configuration 1. In the other configurations studied, the spectra are graphically similar and are not shown. The spectra for the fuel and the moderator near the fuel are similar, with a higher contribution in fast neutrons than thermal neutrons. The reflector water spectra are similar, with a higher contribution in thermal neutrons than fast neutrons.
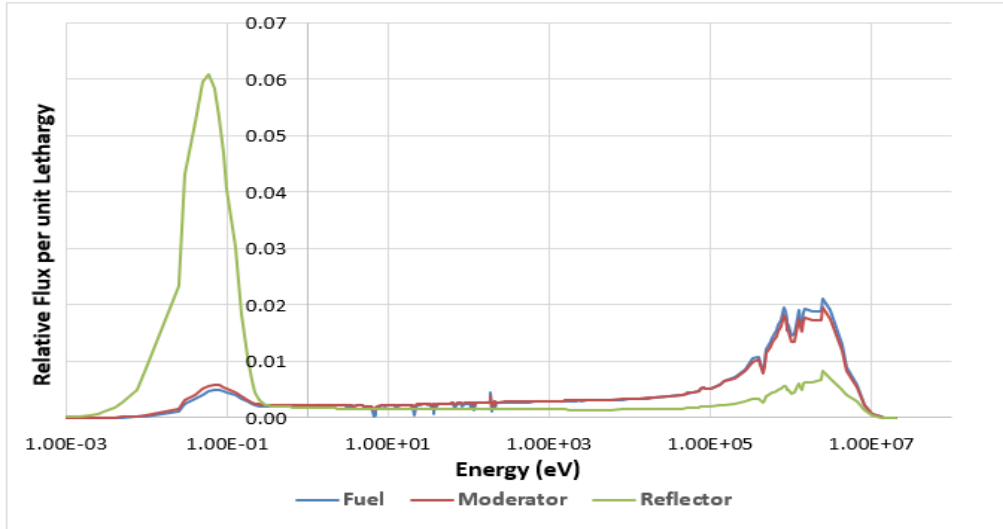
Figure 36: Comparison of the neutron spectra in different locations of configuration 1.

Table 17 compares the neutron fission fraction converted to a three-group energy structure (i.e., thermal, intermediate, and fast). The same energy structure is used that was used in previous publications [5, 6]. Results are given for all ten configurations. With increased neutron absorber plate size and reduced central water channel size, the fissions are less and less thermalized, but the changes are minor at only a few percent. Between each plate, the fissions occur at very similar energies

Table 17. Energy breakdown of fissions events for all ten configurations.

Configuration	Thermal (%)[1]	Intermediate (%)[2]	Fast (%)[3]
1	82.9	11.7	5.4
2	82.9	11.7	5.4
3	82.9	11.7	5.4
4	82.1	12.4	5.6
5	82.2	12.3	5.5
6	82.3	11.7	5.4
7	80.7	13.4	5.9
8	80.9	13.3	5.8
9	81.0	13.2	5.8
10	81.6	12.7	5.7

[1] Thermal: E < 0.625 eV
[2] Intermediate: 0.625 eV < E < 100 keV
[3] Fast: 100 keV < E

6. SENSITIVITY STUDY

CE TSUNAMI 3D is used to calculate sensitivities to k_{eff} for various mixtures, elements, and radioisotopes in different critical configurations. Instead of calculating the sensitivities of the ten configurations, only the most different configurations are studied. Focusing on configurations 1, 4, 7, and 10 is a good way to cover the different sensitivities of the system, as the size of the Boralcan plate and most importantly the size of the central water channel is changed between configurations 1, 4, and 7, and configuration 10 uses the circular water region instead of a water channel. Note that the plate size and water channel size are correlated, so it is not possible to explain the separate contributions of those two parameters changes to any sensitivity change. The following tables show the most sensitive results, always with neutron absorber-related sensitivities (Boralcan and ^{10}B). All TSUNAMI sensitivity results in this section were checked with direct perturbations calculations.

The calculated sensitivity of k_{eff} to mixture is shown in Table 18. Overall, the mixture sensitivities are mostly similar between configurations. The most notable observations are as follows:
- In all configurations, the most sensitive mixture is water, followed by UO_2 fuel.
- The sensitivity to Boralcan is low, meaning a small relative difference in the plate density has a smaller relative influence on k_{eff}.
- The Boralcan absolute value sensitivity increases with increasing plate size.
- The water sensitivity increases with increasing plate size.
- The fuel cladding sensitivity increases with increasing plate size.

Table 18. TSUNAMI sensitivity results by mixture for configurations 1, 4, 7, and 10.

Material	Configuration 1		Configuration 4		Configuration 7		Configuration 10	
	Sensitivity	Uncertainty	Sensitivity	Uncertainty	Sensitivity	Uncertainty	Sensitivity	Uncertainty
UO_2 fuel	9.49E-02	1.3%	9.60E-02	1.3%	8.96E-02	1.5%	9.11E-02	1.4%
Fuel Cladding	3.03E-03	11.7%	3.98E-03	9.2%	4.26E-03	9.0%	4.58E-03	8.2%
Boralcan	-8.39E-04	4.9%	-5.89E-03	1.9%	-9.84E-03	1.5%	-6.29E-04	5.1%
Water	3.10E-01	2.2%	3.53E-01	1.6%	3.99E-01	1.3%	3.31E-01	1.9%

In the following calculation, the focus is on water. Similarly to a previous study [15], the water mixture has been separated into three different regions, as shown in Figure 37. The moderator region is defined as the water between the fuel rods, the central water corresponds to the water channel or central region where the Boralcan plate is located, and the reflector is the water region outside the array of fuel rods. The calculated sensitivity of k_{eff} to water is shown in Table 19. Overall, the mixture sensitivities are mostly similar between configurations. The most notable observations are as follows:
- In all configurations, the most sensitive water region is the moderator region.
- The moderator region sensitivity increases with increasing plate size and decreasing water channel width.
- The central water region sensitivity increases with increasing plate size and decreasing water channel width. It is negative in configurations 1, 4, and 10 and positive in configuration 7. The uncertainty of those results is high, so there is less confidence.
- The reflector region sensitivity increases with increasing plate size and decreasing water channel width.
- The fuel cladding sensitivity increases with increasing plate size.
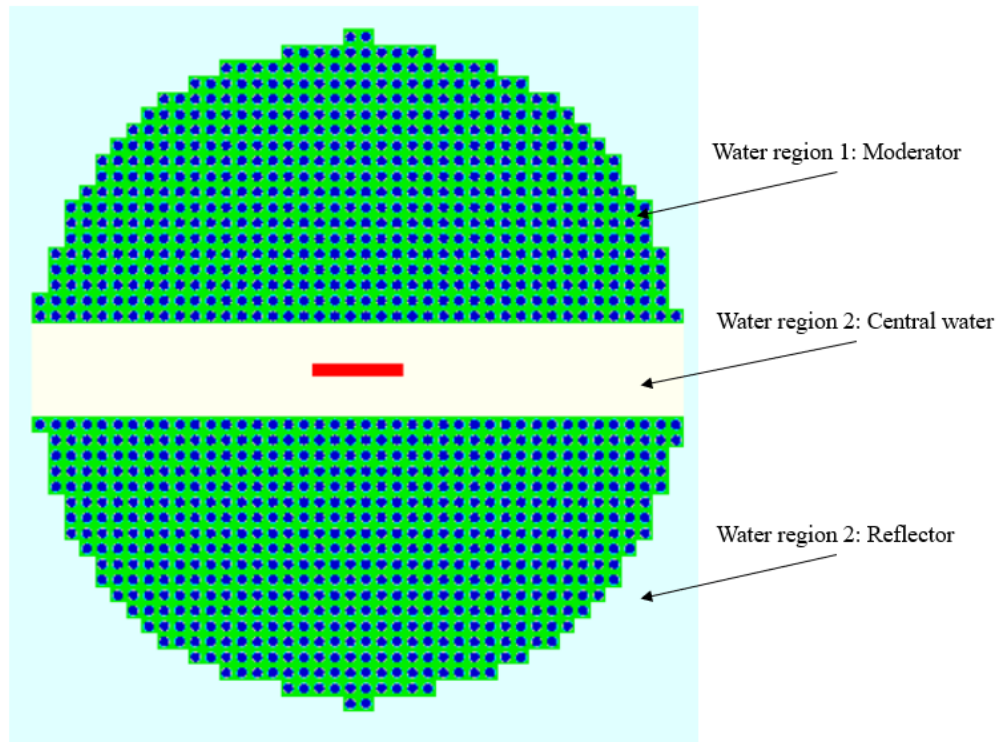
Figure 37. Water regions separation for sensitivity study.

Table 19. TSUNAMI sensitivity results in different water regions for configurations 1, 4, 7, and 10.

Material	Configuration 1 Central water channel width of 5.13 cm		Configuration 4 Central water channel width of 3.42 cm		Configuration 7 Central water channel width of 1.71 cm		Configuration 10 Central water region diameter of 11.97 cm	
	Sensitivity	Uncertainty	Sensitivity	Uncertainty	Sensitivity	Uncertainty	Sensitivity	Uncertainty
Moderator	3.05E-01	1.0%	3.36E-01	0.9%	3.49E-01	0.9%	3.48E-01	0.9%
Central water	-2.00E-02	-24.3%	-6.26E-03	-45.7%	1.28E-02	11.0%	-5.38E-02	-7.8%
Reflector	2.46E-02	14.7%	2.37E-02	15.8%	3.66E-02	10.9%	3.65E-02	10.0%

Isotopes' sensitivity to k_{eff} calculations results are shown in Table 20. Overall, the isotopes' sensitivities are mostly similar between configurations. The sensitivity results obtained for hydrogen in the reflector region are removed because of the overly high uncertainty obtained in some configurations. The most notable observations are as follows:

- In all configurations, the most sensitive isotope is hydrogen in water, followed by [235]U in fuel.
- The [10]B sensitivity is low.
- The [10]B absolute value sensitivity increases with increasing plate size.
- The [238]U sensitivity increases with increasing plate size.
- The hydrogen in moderator sensitivity increases with increasing plate size.
- The oxygen in reflector sensitivity increases with increasing plate size.

Table 20. TSUNAMI sensitivity results of the most sensitive isotopes for configurations 1, 4, 7, and 10.

Material	Configuration 1		Configuration 4		Configuration 7		Configuration 10	
	Sensitivity	Uncertainty	Sensitivity	Uncertainty	Sensitivity	Uncertainty	Sensitivity	Uncertainty
^{16}O in fuel	1.51E-02	4.4%	1.70E-02	4.0%	1.57E-02	4.4%	1.73E-02	3.9%
^{235}U in fuel	1.29E-01	0.6%	1.29E-01	0.6%	1.27E-01	0.6%	1.23E-01	0.6%
^{238}U in fuel	-4.71E-02	1.6%	-4.80E-02	1.7%	-5.11E-02	-1.6%	-4.69E-02	1.7%
H in moderator	2.79E-01	1.1%	3.07E-01	1.0%	3.22E-01	0.9%	3.18E-01	0.9%
^{16}O in moderator	2.67E-02	2.9%	2.84E-02	2.8%	2.73E-02	3.1%	2.96E-02	2.7%
^{16}O in reflector	3.32E-02	1.1%	3.44E-02	1.1%	3.76E-02	1.1%	3.74E-02	1.1%
^{10}B in Boralcan	-8.64E-04	1.8%	-5.84E-03	0.7%	-9.98E-03	0.5%	-5.82E-04	2.2%

7. EXPERIMENT UNCERTAINTIES

In this section, the preliminary experimental uncertainties are evaluated. The designed experiments are similar to the previously thoroughly evaluated lattice configurations found in the ICSBEP Handbook or other IERs currently being designed. In particular, case 9 from the IER-304 CED-2 report involves the 7uPCX fuel rods with a 0.855 cm pitch and a central water channel of 6-rod rows. The only difference from the first nine configurations designed in this report is the addition of the neutron absorber plate in the center. Therefore, the derived experimental uncertainties obtained at 25 ºC in case 9 of the IER-304 CED-2 report are used. Only experimental uncertainties related to the neutron absorber plate are explicitly evaluated in this work and added in quadrature to the total experimental uncertainty. The experimental uncertainties are only evaluated for configuration 1. The experimental uncertainties for parameters not related to the neutron absorber plate for configuration 1, and all the experimental uncertainties for the other configurations will be evaluated in the CED-2 phase. The additional parameter uncertainties are expected to be close to or lower than that derived here for configuration 1.

The experimental uncertainties for the parameters related to the neutron absorber plate are calculated with KENO V.a and are shown in Table 21. Most of the measurement uncertainties are higher than that which can be obtained after the characterization of the plate, so the values shown here are expected to be conservative and will probably be lower in the subsequent phases of the IER. The plate dimension uncertainties are obtained from e-mail communication with MSC [16]. The plate position uncertainties of 1 cm will likely be significantly lower at the SPRF/CX facility, but their influence on k_{eff} is low. The plate density uncertainty is obtained from a method similar to that described in the ICSBEP guide to the expression of uncertainties [17]. The uncertainty in the boron and ^{10}B contents is chosen to be 0.3%, as described in Figure 10.

Table 21. Experimental uncertainties related to the neutron absorber plate for configuration 1.

Uncertainty source	Uncertainty value	Sensitivity		Δk_{eff}
		Value	Uncertainty	
Boralcan density (g/cm3)	0.3588	-3.80E-04	14%	0.00014
Boralcan width (cm)	0.1833	-1.20E-03	35%	0.00022
Boralcan length (cm)	0.1833	-1.13E-03	12%	0.00021
Boralcan thickness (cm)	0.0075	-1.67E-02	42%	0.00001
Boralcan position x (cm)	1	Negligible	Negligible	0.00000
Boralcan position y (cm)	1	Negligible	Negligible	0.00000
Boralcan position z (cm)	1	Negligible	Negligible	0.00000
Boralcan B content (atoms/b-cm)	4.18E-05	-2.09E-01	48%	0.00001
Boralcan ^{10}B content (atoms/b-cm)	1.05E-05	-3.00E-01	13%	0.00005
Boralcan Ti content (atoms/b-cm)	5.64E-07	Negligible	Negligible	0.00000
Boralcan Al content (atoms/b-cm)	5.01E-04	-3.11E-02	91%	0.00002

Table 22 gives the expected benchmark k_{eff} uncertainties in configuration 1 using the previously derived uncertainties from IER-304 CED-2 report case 9 at 25 ºC and the additional uncertainties linked to the addition of the neutron absorber plate in the assembly. The experimental uncertainty increased from 80 to 87 pcm. The addition of the neutron absorber plate only adds seven pcm to the total experimental

uncertainty. Based on these results, the uncertainty of the conceptually designed experiments described in this report are considered low enough to be pursued.

Table 22. Estimated preliminary experimental uncertainties for configuration 1.

Uncertainty source	Configuration 1 Δk_{eff}
Clad inner diameter	0.00001
Fuel outer diameter	0.00000
Upper reflector thickness	0.00000
Fuel Rod UO_2 Mass	0.00002
Fuel rod pellet stack height	0.00004
Fuel Enrichment	0.00012
^{234}U	0.00001
^{236}U	0.00001
Fuel stoichiometry	0.00056
Impurities of the UO_2 Fuel	0.00008
Fuel clad composition	0.00017
Aluminum grid plate composition	0.00002
Water composition	0.00011
Pitch	0.00043
Clad outer diameter	0.00010
Temperature	0.00027
Boralcan density (g/cm3)	0.00014
Boralcan width (cm)	0.00022
Boralcan length (cm)	0.00021
Boralcan thickness (cm)	0.00001
Boralcan position x (cm)	0.00000
Boralcan position y (cm)	0.00000
Boralcan position z (cm)	0.00000
Boralcan B content	0.00001
Boralcan B-10 content	0.00005
Boralcan Ti content	0.00000
Boralcan Al content	0.00002
Sum in quadrature	**0.00087**

8. EXPECTED COST OF THE EXPERIMENTS

The only physical additions required to conduct the designed experiments with a neutron absorber plate placed in the assembly are to obtain the plates and to design and implement a method to support the rods to be stationary in the assembly. The plates will likely require a storage location in the SPRF/CX building, but no specific storage is needed, as the plates are not a sensitive, hazardous, or radioactive material. The neutron absorber plates used in the ten configurations described in this report are small and do not require much work from MSC before being sold, so the cost will be lower than expected. MSC provided a budgetary quote for 27 plates, 3 for each dimension/composition combination. Having three plates for each configuration allows for more options to check the uniformity of the B_4C particles in the plates and will be helpful if any issue or damage appears on the plates. An excerpt of the quote is shown in Figure 38. The shipping cost can be eliminated, because ORNL will obtain the plates directly from MSC in Oak Ridge, Tennessee. The other cost of this experiment is the characterization of the plates. According to internal communication with a different division in ORNL, the use of an x-ray CT system should be free of charge. The spectrometry must be investigated to ensure the estimated cost. Besides these items, the remaining cost is the shipping/delivery of the plates to SNL, with a potential additional specific cost to allow the entry of the plates on site and the labor to perform the experiments. The experiments are expected to have a significant duration because of the time that may be needed to swap the plates from the assembly between each configuration.

1	NEUTRON ABSORBER SAMPLES FROM W1100N.16B WITH DIMENSIONS OF 0.75cm x 5cm X 5cm	3	$	266.00	$	798.00
2	NEUTRON ABSORBER SAMPLES FROM W1100N.16B WITH DIMENSIONS OF 0.75cm X 15cm X 15cm	3	$	271.67	$	815.00
3	NEUTRON ABSORBER SAMPLES FROM W1100N.16B WITH DIMENSIONS OF 0.75cm X 20cm X 20cm	3	$	273.67	$	821.00
4	NEUTRON ABSORBER SAMPLES FROM W1100N.23B WITH DIMENSIONS OF 0.30cm X 5cm X 5cm	3	$	275.33	$	826.00
5	NEUTRON ABSORBER SAMPLES FROM W1100N.23B WITH DIMENSIONS OF 0.30cm X 15cm X 15cm	3	$	277.33	$	832.00
6	NEUTRON ABSORBER SAMPLES FROM W1100N.23B WITH DIMENSIONS OF 0.30cm X 20cm X 20cm	3	$	279.33	$	838.00
7	NEUTRON ABSORBER SAMPLES FROM W1100N.17B WITH DIMENSIONS OF 0.17cm X 5cm X 5cm	3	$	348.33	$	1,045.00
8	NEUTRON ABSORBER SAMPLES FROM W1100N.17B WITH DIMENSIONS OF 0.17cm X 15cm X 15cm	3	$	350.33	$	1,051.00
9	NEUTRON ABSORBER SAMPLES FROM W1100N.17B WITH DIMENSIONS OF 0.17cm X 20cm X 20cm	3	$	352.33	$	1,057.00
10	SHIPPING OF 27 NEUTRON ABSORBER SAMPLES FROM MSC TO ORNL	1	$	891.00	$	891.00
				TOTAL	$	8,974.00

Figure 38. Budgetary quote excerpt for 27 neutron absorber plates provided by MSC.

A list of all the potential additional equipment with the associated cost estimate needed for this experiment is shown in Table 23. Currently, the only equipment required is the plates, plate support, and storage. Additional work and consultation with the experiment team are needed to determine if other equipment is required. The cost estimates include acquiring the materials, manufacturing, installation labor, and other considerations.

Table 23. Potential additional equipment and experiment cost.

Equipment	Total Cost Estimate (material, manufacturing, labor, etc.)
27 neutron absorber plates (MSC)	$8083 + $labor
Rods support	$design + $material + $manufacture + $labor
Plates and plates support storage	$material + $manufacture
X-ray CT scan	$0
Density, elemental/isotopic characterization	No estimate obtained
Shipping/delivery/entry on site	$labor

9.   BIASES

The proposed experiments are expected to behave in a manner similar to those documented in LCT078, LCT079, and some future experiments designed in IER-304. A potential bias may appear if the plates do not have a good B_4C particle uniformity, so the experimenters should keep track of each plate, even those that are theoretically the same (dimensions and B_4C concentration).

10. COMPLIANCE WITH C$_E$DT MANUAL REQUIREMENTS

Table 5.1 in the C$_E$dT manual [9] provides an example of required input and calculated values for the design, execution, and documentation of criticality (k$_{eff}$) measurement experiments. Table 24 replicates the table's columns from the C$_E$dT manual applicable to the current CED-1 status. Brief explanations related to this IER are also included.

Table 24. C$_E$dT manual example requirements for CED-1 of a criticality measurement experiment.

Input parameters	Preliminary design CED-1	Notes
Masses (m, σ_m)	✓	Most values and uncertainties are included in the LCT078 and LCT102 evaluations, and estimations are given for the neutron absorber plates.
Compositions (N, σ_N)	✓	Most values and uncertainties are included in the LCT078 and LCT102 evaluations, and estimations are given for the neutron absorber plates.
Dimensions (x, σ_x)	✓	Most values and uncertainties are included in the LCT078 and LCT102 evaluations, and estimations are given for the neutron absorber plates.
Positions (y, σ_y)	✓	Most values and uncertainties are included in the LCT078 and LCT102 evaluations, and estimations are given for the neutron absorber plates.
Calculated parameters	**Preliminary design CED-1**	**Notes**
Eigenvalue (k$_{eff}$, σ_k)	✓	Experiment k$_{eff}$ and uncertainties are estimated above.
Material worth (Δk$_{eff}$, $\sigma_{\Delta k}$)[a]	✓[a]	Material sensitivities are discussed above.
Neutron energy spectrum	✓	The neutron energy spectra are discussed above.
Neutron balance (by isotope, region)[b, c]	✓[c]	Not needed.
Isotope sensitivities (by reaction)[c]	✓[c]	Isotope sensitivities are addressed above.

Note: Columns 1 and 2 and footnotes a–c are from [9, Table 5.1].
[a] If relevant.
[b] Production, absorption, and leakage fractions.
[c] Perhaps not required, but desirable.

11. CONCLUSION

IER-554 considers critical experiments based on assemblies using the 7uPCX fuel rods with the insertion of neutron absorber plates in their centers. Ten different array configurations associated with nine neutron absorber plates of different dimensions and B_4C concentrations are proposed, providing opportunities to analyze different sensitivities to k_{eff}. The analysis shows that such experiments can be performed with acceptably low k_{eff} uncertainties. The k_{eff} uncertainty can be further reduced by adequately characterizing the neutron absorber plates. The sensitivity results obtained with TSUNAMI calculations show the experiments have a low differential k_{eff} sensitivity to the neutron absorber plates, but the integral sensitivity is high. In the next phase CED-2, data adjustment techniques will be explored to further demonstrate the worth of performing those experiments for nuclear data testing.

12. REFERENCES

1. *Standard Review Plan for Spent Fuel Dry Storage Systems and Facilities*, NUREG-2215, US Nuclear Regulatory Commission (2020).
2. *International Handbook of Evaluated Criticality Safety Benchmark Experiments*, NEA/NSC/DOC(95)03, NEA Nuclear Science Committee (2016).
3. S. Gunji, "TRACY: Unreflected 10%-Enriched Uranyl Nitrate Solution in a 50-cm-Diameter Annular Tank," (LEU-SOL-THERM-13), *International Handbook of Evaluated Criticality Safety Benchmark Experiments*, Organisation for Economic Co-operation and Development, Nuclear Energy Agency, Paris, France, NEA/NSC/DOC(2006)1 (2019).
4. H. Akhurt, *Handbook of Neutron Absorber Materials for Spent Nuclear Fuel Storage and Transportation Applications*, 3002018496, EPRI, Palo Alto, CA (2021).
5. G. A. Harms, "Water Moderated Square-Pitched U(6.90)O2 Fuel Rod Lattices with 0.52 Fuel-to-Water Volume Ratio," (LCT-078), *International Handbook of Evaluated Criticality Safety Benchmark Experiments*, Organisation for Economic Co-operation and Development, Nuclear Energy Agency, Paris, France, NEA/NSC/DOC(2006)1 (2013).
6. D. E. Ames and G. A. Harms, *Pitch Variation Experiments in Water-Moderated Square-Pitched U(6.90)O2 Fuel Rod Lattices with Fuel to Water Volume Ratios Spanning 0.08 TO 0.67*, IER-230 CED-4a report, Sandia National Laboratory, Albuquerque, NM (2020).
7. J. B. Clarity, R. C. Gallagher, M. N. Dupont, and C. W. Chapman, *Integral Experiment Request 304 CED-2 Summary Report*, ORNL/TM-2021/1905, Oak Ridge National Laboratory, Oak Ridge, TN (2021).
8. J. B. Clarity, D. E. Mueller, W. J. Marshall, and R. M. Westfall, *Integral Experiment Request 441 CED-1 Summary Report*, ORNL/TM-2017/214, Oak Ridge National Laboratory, Oak Ridge, TN (2017).
9. D. G. Bowen, *Critical and Subcritical Experiment Design Team (CEdT) Process Manual of the United States Department of Energy Nuclear Criticality Safety Program*, Revision 1 (2016). https://ncsp.llnl.gov/sites/ncsp/files/2021-04/NCSP_Manual_REV1_Final.pdf
10. Rio Tinto. "About," accessed September 17, 2022. https://www.riotinto.com/about
11. Manufacturing Sciences Corporation. "Our Business," accessed September 17, 2022. https://www.mfgsci.com/overview\
12. J. Jansen, Manufacturing Sciences Corporation, Neutron absorber small sample potential procurement, Personal Communication (2022).
13. P. Bingham, Oak Ridge National Laboratory, NDA for Neutron Absorber B_4C Plates, Personal Communication (2022).
14. Obtained from E. Cakmak, Oak Ridge National Laboratory, CT system picture, Personal Communication (2022).
15. M. N. Dupont and T. M. Miller, *Integral Experiment Request 304 CED-1 Summary Report*, ORNL/SPR-2017/485, Oak Ridge National Laboratory, Oak Ridge, TN (2017).
16. B. Holley, Manufacturing Sciences Corporation, Neutron absorber small sample potential procurement, Personal Communication (2022).
17. V. F. DEAN, Ed., "ICSBEP Guide to the Expression of Uncertainties," NEA/NSC/DOC(95)03, Organisation for Economic Co-operation and Development - Nuclear Energy Agency, Paris, France (2019).